Arch. Metall. Mater., Vol. 61 (2016), No 1, p. 143–148

DOI: 10.1515/amm-2016-0026

K. ŻABA*,# S. PUCHLERSKA*, M. KWIATKOWSKI*, M. NOWOSIELSKI*, M. GŁODZIK*, T. TOKARSKI*, P. SEIBT*

COMPARATIVE ANALYSIS OF PROPERTIES AND MICROSTRUCTURE OF THE PLASTICALLY DEFORMED ALLOY INCONEL®718, MANUFACTURED BY PLASTIC WORKING AND DIRECT METAL LASER SINTERING

Nickel superalloys as Inconel® are materials widely used in the aerospace industry among others for diffusers, combustion chamber, shells of gas generators and other. In most cases, manufacturing process of those parts are used metal strips, produced by conventional plastic processing techniques, and thus by hot or cold rolling. An alternative technology allowing for manufacturing components for jet engines is the technique of 3D printing (additive manufacturing), and most of all Direct Metal Laser Sintering, which is one of the latest achievement in field of additive technologies.

The paper presents a comparative analysis of the microstructure and mechanical properties of the alloy Inconel®718 manufactured by plastic working and Direct Metal Laser Sintering technology, in the initial state, after deformation and after heat treatment.

1. Introduction

Nickel superalloys as Inconel® are materials widely used in the aerospace industry among others for diffusers, combustion chamber, shells of gas generators and other, exposed to high temperature and pressure [1-3].

The microstructure of Inconel superalloy is characterized by a multi-component, complex morphology, crucial for their specific properties. The main alloying elements, addition of nickel, are: 10-20% Cr, 6% Al and Ti, 5-10% Co and Bo, Zr, C, Mo, W, Nb, Ta and Hf. Other ingredients are additives, which the content is strictly defined. The influence of alloying elements on the various properties of materials such as Inconel are shown in Refs [4-7]. The connection between the microstructure of a nickel superalloy, and their final properties are well known in the range from ambient temperature to 1100°C [8].

The components of aircraft engines have often complicated construction, therefore production of these parts requires the designing of advanced metal forming processes [9]. The task is complicated because of specific technological properties of Inconel® alloy, like deformation resistance, high intensity of strengthening and high recrystallization temperature [10]. In industrial conditions, for demanding applications of aerospace industry, Inconel®718 alloy is used in the form of sheet, produced through cold or hot rolling. In addition to conventional methods of forming, for manufacture these kind of products are used flow and share forming [11-12]. The processes are carried out to the cold and hot with use of local laser heating. Despite the advanced level of knowledge of the process, during production are observed a number of defects, arising from the nature of the process and from the state of structure of deformed material either. In semi-finished products are observed: corrugation or cracks of the flange, peripheral cracks, pasting material on the forming tool [13].

Chance for an alternative to traditional methods of production and processing hard-formable alloys is additive manufacturing technology [14]. The latest achievement of additive technologies is the Direct Metal Laser Sintering (DMLS) technique. The process involves melting and bonding together successive layers of metal powder, using laser. Process is based on the CAD model. The final surface treatment of the material is reduced to a minimum or not required. The main advantages of DMLS technology are excellent dimensional accuracy, the ability to produce complex parts that do not require post-processing, a unique surface quality and excellent mechanical properties. The technology enables production of products made of iron, titanium and nickel alloys. Detailed information on this technology are presented in Refs [15,16].

The article presents a comparative analysis of the microstructure and mechanical properties of Inconel® 718 superalloy, produced by conventional plastic forming technology and using DMLS in initial state, after plastic forming in the different degrees of deformation and after heat treatment.

2. Experimental procedure

For research were chosen two Inconel®718 materials, with a thickness of 2.15 mm, produced by various methods. The first is the plate (Fig. 1a), produced by conventional rolling (later in the article referred to as PF) and the second material is a plate (Fig. 1b), made by DMLS.

* AGH UNIVERSITY OF SCIENCE AND TECHNOLOGY, FACULTY OF NON-FERROUS METALS, AL. MICKIEWICZA 30, 30 – 059 KRAKOW, POLAND

Corresponding author: krzyzaba@agh.edu.pl

a) b)

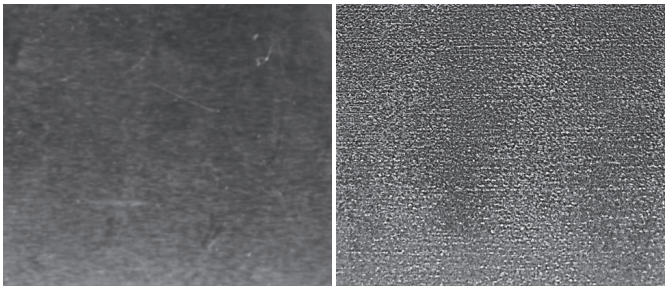

Fig. 1. Samples for research a) PF, b) DMLS

To produce DMLS plates used heat and corrosion resistant powder EOS NickelAlloy IN718, with a grain size of ~36 µm, optimized for processing in EOSINT M systems in DMLS technology and a printer EOSINT M EOS 280. Printer specifications is shown in Ref. [17].

Next PF and DMLS samples were subjected to rolling, which realized on the quarto reversing mill. Both types of samples cut parallel and perpendicular to the direction of rolling and to the direction of movement of the laser beam, were deformed with various degrees of deformation: 15, 30 and 50%.

The next step was heat treatment on the plastically deformed materials, realized according to the standard [18] in two steps:

1. Solution annealing at 980 °C for 1 hour, cooled in H_2O.
2. Aging at 720 °C for 8 hours, furnace cooling to 620 °C, holding at 620 °C for 18 hours.

The chemical composition of PF and DMLS samples in the initial state was analysed using the Inductively Coupled Plasma (ICP) method [19-20]. Further tests were carried out on PF and DMLS samples in the initial state, after deformation and after heat treatment.

At first was determined the mechanical properties of samples in a uniaxial tensile test, carried out according to standard [21]. The study used a static testing machine Zwick/Roell Z050, equipped testXpert® II program, used for control and data acquisition. The results allowed to determine the strengthening properties (UTS and YS0.2) and plastic properties (A) of tested materials.

Then the surface roughness test was performed, according to standard [22], using an optical profilometer Veeco Wyko NT9300. Area of sampling was 3.65 µm.

In last step were made microstructural observations (SEM), X-ray microanalysis on a Hitachi scanning electron microscope SU-70 and X-ray phase analysis using D8 ADVANCE diffractometer.

The test results are shown in tables, in the diagrams and photographs.

3. Research results

Chemical composition of PF and DMLS are presented in Table 1.

The results show that the chemical composition of PF and DMLS are comparable. The largest is nickel content of approx. 55%, followed by chromium and iron approx. 20% and molybdenum approx. 2.7%. Other components are present at the level of tenths and hundredths of a percent.

The results of surface roughness for the PF and DMLS samples in initial conditions, after 50% plastic deformation and after heat treatment is shown in Figs 2-4.

The results are presented in the form of 3D profiles and characteristic for measuring of roughness values R_a and R_z.

a) b)

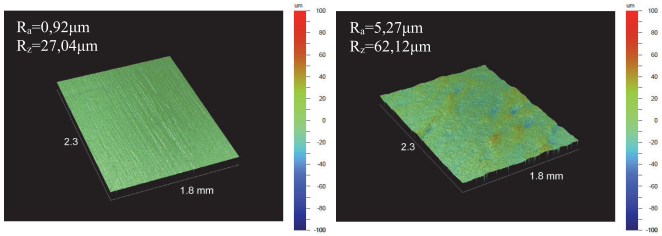

Fig. 2. The surface roughness of the samples PF (a) and DMLS (b) in the initial state

a) b)

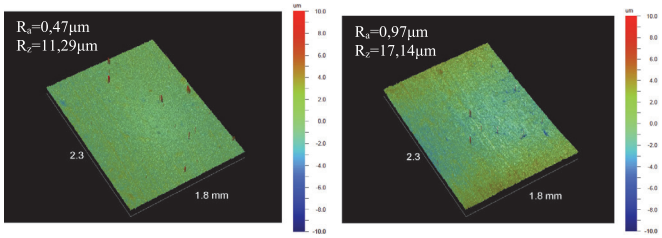

Fig. 3. The surface roughness of the samples PF (a) and DMLS (b) after 50% deformation

a) b)

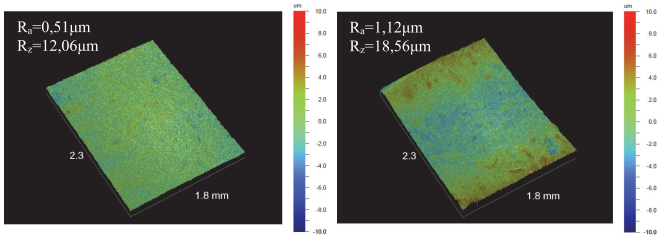

Fig. 4. The surface roughness of the samples PF (a) and DMLS (b) after 50% deformation and heat treatment

TABLE 1

Chemical composition of PF i DMLS samples [%]

Material	Ni	Cr	Nb	Mo	Ti	Al	Co	Mn	Fe
PF	54.87	20.29	3.09	2.68	0.60	0.58	0.37	0.06	bal.
DMLS	54.56	19.95	2.94	2.80	0.78	0.56	0.22	0.03	bal.

PF and DMLS samples in initial conditions has quite different surface roughness. Surface of PF sample is smooth with an average roughness of R_a=0.92 μm and R_z=27.04 μm (Fig. 2a). However the surface of DMLS sample has repeatedly higher average roughness of R_a=5.27 μm and R_z=62.12 μm (Fig. 2b). The reason of this difference is the method of producing materials. PF samples were prepared by rolling, heat treatment and in the final stage of the flattening. DMLS proces causes that the surface roughness is much greater.

The deformation of 50%, causes, that the surface of the PF and DMLS sample is considerably smoothed. The consequence is a reduction in the roughness values, which for PF sample are R_a=0.47 μm and R_z=11.29 μm (Fig. 3a) and for DMLS sample are R_a=0.97 μm and R_z=17.14 μm (Fig. 3b).

Heat treatment has no significant effect on the surface roughness after deformation. However, it should be noted minor increase of roughness parameters which for PF sample are R_a=0.51 μm and R_z=12.06 μm (Fig. 4a), while for the DMLS sample are R_a=1.12 μm and R_z=18.56 μm (Fig. 4b).

The results of the strength (UTS,YS0,2) and plastic (E) properties of PF and DMLS material in the initial state after deformation of 15, 30 and 50% and after the heat treatment is shown in Figs 5, 6.

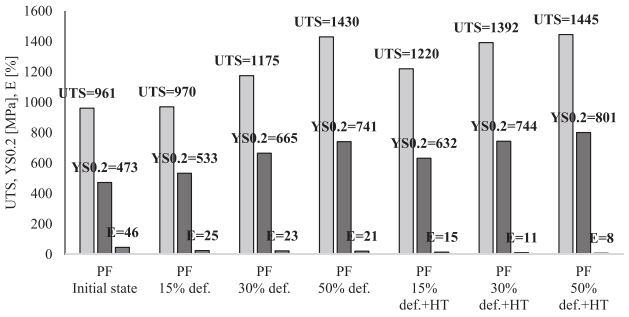

Fig. 5. The results of the mechanical properties of PF samples in the initial state, after deformation of 15, 30 and 50% and heat treatment

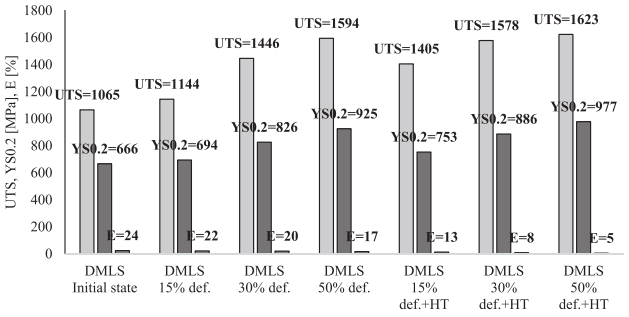

Fig. 6. The results of the mechanical properties of DMLS samples in the initial state, after deformation of 15, 30 and 50% and heat treatment

The results of the mechanical properties of PF and DMLS samples slightly dependent on the direction of sampling relative to the rolling direction and the direction of movement of the laser beam. Therefore, the results are presented as the averages of the strength (UTS,YS0,2) and plastic (A) properties for samples cut in both directions. R_m tensile strength at break, normally a higher value DMLS samples. Is in the range from 1065 MPa to 1623 MPa, and for PF samples is from 961 MPa to 1445 MPa. Obviously, the tensile strength UTS increases with the strengthening of the material for each case. Similarly, the yield strength YS0,2 (Figs 5, 6). The average value YS0,2/UTS for PF samples is $R_{0.2}/R_m$=0.53, while for DMLS samples YS0,2/UTS=0,58. This demonstrates the improved susceptibility to the formability of PF samples.

Elongation A of PF and DMLS samples does not depend on anisotropy. In most cases, the elongation value is greater for PF samples PF. Is in the range from 8 to 46%, and for DMLS samples is from 5 to 24% (Figs 5, 6).

The results of microstructural observation of PF and DMLS samples in the initial state shown in Fig. 7.

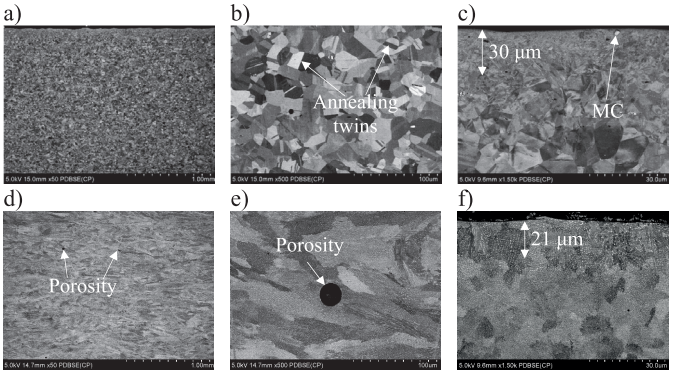

Fig. 7. Microstructure of PF (a-c) and DMLS (d-f)

The structure of PF samples is characteristic of the Inconel superalloy, which was found on the basis of the literature [23]. The microstructure of PF is recrystallized and characterized by grains of clear boundaries. Austenite grains are equiaxed. In the structure was observed annealing twins. The structure of the surface layer (Fig. 6c) is much more fine-grained. This is probably a result of finishing sheet consisting of flattening, it means rolled sheet with little deformation after annealing. The layer thickness is about 30 μm. The matrix of material is austenit, solid solution based on nickel. In the structure there are also isolated MC-type carbides, having a composition rich in niobium.

Microstructure of DMLS samples is characterized by asymmetric, elongated grains (Fig. 7d, f) of the inhomogeneous phase composition. Surface layer of DMLS samples in the initial state (Fig. 7f) are characterized by typical morphological characteristics of dendrites. Interdendritic segregation is the result of rapid crystallization of laser-sintered material at the edges than in the rest of the volume, which results from non-uniform temperature gradient. The layer thickness is approx. 21 μm. The observations indicate that in the structure appear in a few round micropores with size approx. 20 μm.

Figs 8, 9 show the microstructure of the PF and DMLS samples after rolling with deformation of 15, 30 and 50%.

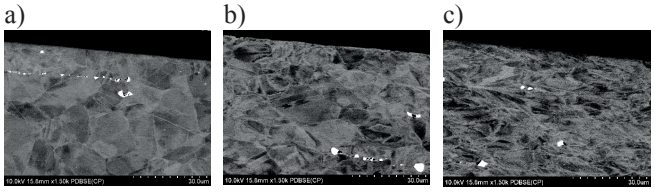

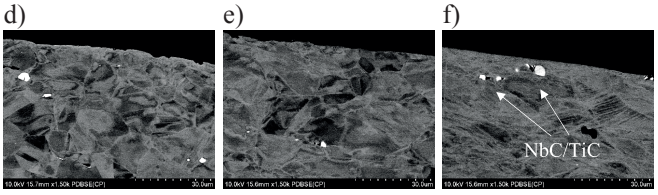

Fig. 8. The microstructure of PF samples cut in the direction parallel (a-c) and perpendicular (d-f) to the direction of rolling, after the deformation of 15% (a, d); 30% (b, e) and 50% (c, f)

After rolling with 15% deformation, the grain boundaries are clearly visible and the grains are deformed slightly (Fig. 8a, d). After 30% deformation, the grain boundaries are still visible and grains are deformed, assuming an elongated shape (Fig. 8b, e). After 50% deformation grain boundaries are difficult to identify and the grains are deformed largely, adopting elongated, symmetrical shape (Fig. 8c, f). The matrix is a multiphase. The microstructure of PF samples has a number of block precipitation, mainly at the surface, contracting along the rolling axis, which can be observed in the photographs depicting PF samples cut in the parallel direction (Fig. 8a, c) to the rolling direction. Precipitation in the form of MC-type carbides are located in a layer with thickness of approx. 12 μm from the surface to the inside of the material. The particles of these phases are rich in niobium and titanium. Also identified oxides Al_2O_3 and Cr_2O_3 typical for this type of alloy [24].

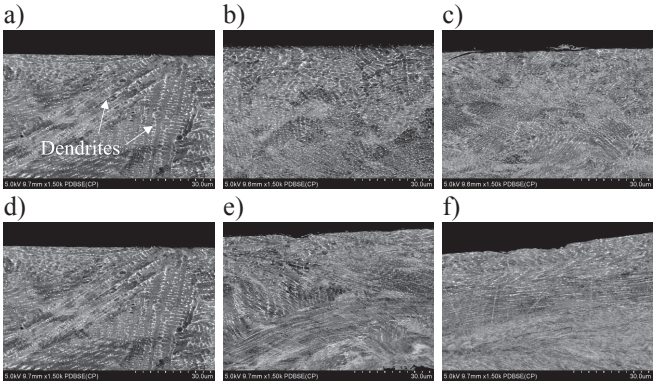

Fig. 9. The microstructure of DMLS samples cut in the direction parallel (a-c) and perpendicular (d-f) to the direction of movement of the laser beam, after the deformation of 15% (a, d); 30% (b, e) and 50% (c, f)

Observation of the microstructure in the surface layer DMLS samples, after rolling with varying degrees of deformation, indicate the presence of characteristic dendrites, which are a result of laser melting (Fig. 9a, d). The dendrites solidify in the direction of the heat source, creating a pattern characteristic of melt or welded surface, which is consistent with the results shown in Refs [25, 26]. Only after the high plastic deformation (Fig. 9c, f) the material loses the characteristic structure.

Figs 10, 11 show microstructure of PF and DMLS samples after rolling with deformation of 15, 30 and 50% and after heat treatment.

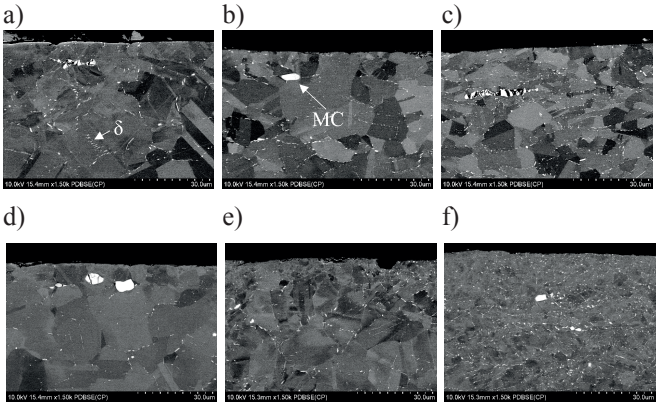

Fig. 10. The microstructure of PF samples cut in the direction parallel (a-c) and perpendicular (d-f) to the direction of rolling, after the deformation of 15% (a, d); 30% (b, e) and 50% (c, f) and after heat treatment

The structure of PF samples after heat treatment (Fig. 10) is characterized by distinct grain boundaries. In the sample (Fig. 10a, d) in which the degree of deformation was smaller, the grain size is larger than the grains in the place where the deformation was higher (Fig. 10c, f). There has been a growth of the matrix grains and partially disappeared a multiphase character. The material has been rebuilding after plastic deformation. Grain boundaries are rich in δ phase [27]. The precipitation of δ phase in the form of thin plates, is carried in the discontinuous reaction, starting at the grain boundaries, and at a later stage in the form of intergranular precipitates. There has been reported [28] that the initial reaction predominates at low temperatures, while the later reaction is more typical of the intermediate temperatures, although there are no complete studies carried out in this aspect. At high temperatures, can be observed both of precipitations, at the grain boundaries and intergranular separation.

Fragmentation and the distribution of carbides have strongly influences at creep strength of the alloy. Fig. 10 showing the MC-type carbides in the form of large precipitates rich in niobium, appearing in the areas inside the austenite grains. These types of carbide are the main phases, precipitated nickel superalloys, the next to γ' phase.

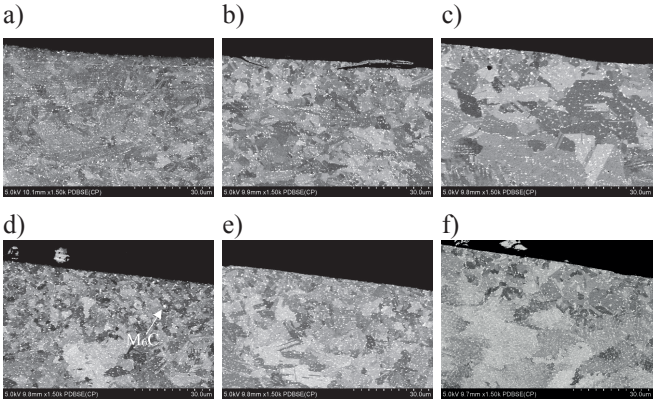

Fig. 11. The microstructure of DMLS samples cut in the direction parallel (a-c) and perpendicular (d-f) to the direction of movement of the laser beam, after the deformation of 15% (a, d); 30% (b, e) and 50% (c, f) and after heat treatment

The microstructure of DMLS samples after heat treatment (Fig. 11) is recrystallized and the dendritic structure disappeared completely. There was a fluctuation of chemical components of the matrix. Grains have clear boundaries, the surface of the material is finer than in the rest of the volume. Recrystallization was more intensive at the surface of the heat treated material. The structure is extremely rich in small, regularly spaced precipitation at grain boundaries. This is probably M_6C-type carbides.

4. Conclusions

Based on research can provide the following conclusions:

1. On the basis of microstructural observations should be concluded that characteristic is the variation of microstructure and grain size of materials made by classic way (PF) in the form of sheet and by using DMLS. DMLS samples have a characteristic structure for melted and sintered material. The structure of PF samples is characterized by a large precipitation of MC-type carbides. After heat treatment the structure of DMLS is richer in precipitation then PF structure.
2. For DMLS additional deformation by rolling is required, because of surface roughness.
3. Material made by DMLS in the initial state has a much higher porosity than PF material in initial state. Cold rolling eliminates porosity of DMLS.
4. Anisotropy does not significantly affect the material properties of both PF and DMLS.

REFERENCES

[1] Q. Huan, Review of INCONEL 718 alloy: its history, properties, processing and developing substitutes, J. Mater. Eng. **8**, 92-100 (2012).

[2] D. Dudzinski, A. Devilleza, A. Moufkia, D. Larrouquèreb, V. Zerroukib, J. Vigneaub, A review of developments towards dry and high speed machining of Inconel 718 alloy, Int. J. Machine Tools Manuf. **44,** 439-456 (2004).

[3] D.F. Paulonis, J.J Schirra, Alloy 718 at Pratt & Whitney – historical perspective and future challenges, superalloys 718, 625, 706 and various derivatives, TMS (2001).

[4] S. Mrowec, T. Werber, Nowoczesne materiały żaroodporne, Wydawnictwa Naukowo- Techniczne, Warszawa, 1982.

[5] B. Mikułowski, Stopy żaroodporne i żarowytrzymałe. Nadstopy, Wydawnictwa AGH, Kraków, 1997.

[6] B. Dubiel, A. Czyrska-Filemonowicz, Żarowytrzymałe stopy umocnione dyspersyjnie cząstkami tlenków (stopy ODS), Inz. Mat. **21** 20-28 (2000)

[7] C.T. Sims, N.S. Stoloff, W.C. Hagel, Superalloys II, Ed. J. Willey & Sons, New York 1987.

[8] J. Eiselstein, D. Pasquine, Phase transformation in nickel-base alloys, International Symposium on Structural Stability in Superalloys, Seven Springs, PA 1968.

[9] T. Drenger, J. Wiśniewski, S. Sosnowski, Ł. Nowacki, T. Gądek, Z. Ulatowski, Rozpoznawcze badania możliwości kształtowania metodami obróbki plastycznej elementów ze stopu niklu Inconel 625, Obróbka Plastyczna Metali **18**, 15-22 (2007).

[10] A. Nowotnik, K. Kubiak, Wpływ parametrów odkształcania na procesy wydzieleniowe w nadstopie niklu typu Inconel, Hutnik – Wiadomości Hutnicze **75**, 432-434 (2008).

[11] M. Pawlicki, Plastyczne kształtowanie metali w technologii zgniatania obrotowego, Kraków 2013.

[12] I. Dul, Zastosowanie i przetwarzanie stopów niklu w przemyśle lotniczym, PS **81,** 67-70 (2009).

[13] O. Music, J.M. Allwood, K. Kawai, A review of the mechanics of metal spinning, J. Mater. Process. Technol. **210,** 3-23 (2010).

[14] J.P. Kruth, M.C. Leu, T. Nakagawa, Progress in additive manufacturing and rapid prototyping, CIRP Ann. Manuf. Techn. **47** (1998) 525-540.

[15] A. Simchia, F. Petzoldt, H. Pohl, On the development of direct metal laser sintering for rapid tooling, J. Mater. Process. Technol. 141 319-328 (2003).

[16] D. Atkinson, Rapid Prototyping and Tooling, A Practical Guide, Strategy Publication Ltd., Welwyn Garden City, UK 1997.

[17] Information on http://www.eos.info/

[18] AMS 5662.

[19] A.A. Ammann, Inductively coupled plasma mass spectrometry (ICP MS): a versatile tool, J. Mass Spectrom. **42**, 419-427 (2007).

[20] R. Knochenmuss, Ion formation mechanisms in UV-MALDI, Analyst **131**, 966-986 (2006).

[21] PN-EN ISO 6892-1:2009.

[22] PN-EN 10049:2008P.

[23] G. Vander Voort, Metallography of superalloys, Industrial Heating **70**, 40-43 (2003).

[24] G. Appa Rao, K. Satya Prasad, M. Kumar, M. Srinivas, D. S. Sarma, Effect of standard heat treatment on the microstructure and mechanical properties of hot isostatically pressed superalloy inconel 718, J. Mater. Sci. Technol. **19**, 1-9 (2003).

[25] S.A. David, S.S. Babu, J.M. Vitek, Welding: Solidification and microstructure, JOM – J. Min. Met. Mat. Soc. **55**, 14-20 (2003).

[26] K.A. Mumtaz, P. Erasenthiran, N. Hopkinson, High density selective laser melting of Waspaloy (R), J. Mater. Process. Tech. **195,** 77-87 (2008)

[27] M. Dehmas, J. Lacaze, A. Niang, B. Viguier, TEM Study of high-temperature precipitation of delta phase in Inconel 718 alloy, Adv. Mater. Sci. Eng. 2011 (2011) 1-9.

[28] I. Kirman, D.H. Warrington, The precipitation of Ni_3Nb phases in a Ni-Fe-Cr-Nb alloy, Metall. Mater. Trans. B **1**, 2667-2675.

Received: 20 February 2015.